SPECIFIC SENSORY NEURONS AND INSULIN-LIKE PEPTIDES MODULATE FOOD TYPE-DEPENDENT OOGENESIS AND FERTILIZATION IN *CAENORHABDITIS ELEGANS*

Shashwat Mishra[1], Kelsey Marbach[1], Mohamed Dabaja[1], Asra Akhlaq[1], Mediha Rovcanin[1], Bianca Pereira[1], Rashmi Chandra[1], Antonio Caballero[2], Diana Fernandes de Abreu[2], QueeLim Ch'ng[2], Joy Alcedo[1,*]

[1]Department of Biological Sciences, Wayne State University, Detroit, Michigan, USA

[2]Centre for Developmental Neurobiology, King's College London, London, UK

*Correspondence to: joy.alcedo@wayne.edu

Abstract

An animal's responses to environmental cues are critical for its reproductive program. Thus, a mechanism that allows the animal to sense and adjust to its environment should make for a more efficient reproductive physiology. Here we demonstrate that in *Caenorhabditis elegans* specific sensory neurons influence onset of oogenesis through insulin signaling in response to food-derived cues. The chemosensory neurons ASJ modulate oogenesis onset through the insulin-like peptide (ILP) INS-6. In contrast, other sensory neurons, the olfactory neurons AWA, regulate food type-dependent differences in *C. elegans* fertilization rates, but not onset of oogenesis. This AWA effect is distinct from the effects of insulin receptor signaling, where the latter regulates fertilization independently of food type and requires ILPs other than INS-6. Together our findings suggest that optimal reproduction requires the integration of diverse food-derived inputs through multiple neuronal signals acting on the *C. elegans* germline.

Introduction

The survival of an individual and its species involves reproductive mechanisms that are subject to food-dependent modulation. In the worm *C. elegans*, sensory neurons influence food-dependent survival (***Maier et al., 2010***) and germline physiology (***Dalfo et al., 2012; Sowa et al., 2015; Aprison and Ruvinsky, 2017; Perez et al., 2021***). This suggests the intriguing possibility that sensory perception optimizes survival by modulating the germline in a given environment, which makes it important to understand how the sensory system affects germ cells.

In the germline of the *C. elegans* hermaphrodite, germ cells first undergo spermatogenesis, before switching to oogenesis [***Figure 1A***; reviewed by (***Kimble and Crittenden, 2007***)]. After oogenesis begins, oocytes undergo arrest at the diakinesis stage of prophase I [reviewed by (***Greenstein, 2005***)]. Oocytes are released from this arrest in an assembly-line manner by a hormone secreted from sperm, where the oocyte most proximal to the spermatheca matures first (***McCarter et al., 1999; Miller et al., 2001***). Once released from arrest, the oocyte is also immediately ovulated into the spermatheca, where it is fertilized by a sperm (***McCarter et al., 1999; Miller et al., 2001***). Thus, in *C. elegans* hermaphrodites, the rate of oocyte maturation determines the rate of fertilization (***McCarter et al., 1999***).

Some of the *C. elegans* sensory neurons have been shown to modulate germ cell proliferation (***Dalfo et al., 2012; Aprison and Ruvinsky, 2017***) and oocyte senescence (***Sowa et al., 2015***) in response to food or pheromones. However, it remains unclear whether the same sensory neurons regulate germline differentiation and fertilization or what signaling mechanisms underlie these sensory influences.

Insulin signaling could mediate the sensory responses to food [reviewed by (***Allen et al., 2015***)]. Worms have 40 insulin-like peptides [ILPs; (***Duret et al., 1998; Kawano et al., 2000; Pierce et al., 2001; Li et al., 2003***), many of which are expressed in sensory

neurons and could act alone or combinatorially to regulate several physiological programs (***Cornils et al., 2011; Chen et al., 2013; Ritter et al., 2013; Fernandes de Abreu et al., 2014***). Indeed, two ILPs, *ins-3* and *ins-33*, have already been shown to regulate germ cell proliferation (***Michaelson et al., 2010***); however, the cells that secrete these signals that affect the germline are unknown.

In this study, we find that specific sensory neurons and ILPs regulate onset of oogenesis and fertilization through food type-dependent and -independent mechanisms. In response to a specific food type, we show that the chemosensory neuron ASJ modulates oogenesis onset. This ASJ-dependent effect on oogenesis involves ASJ-specific expression of the ILP *ins-6*. In contrast, an olfactory neuron, AWA, regulates food type-dependent fertilization rates through mechanisms that differ from insulin receptor signaling. The insulin receptor pathway alters fertilization rates independent of food cues and employs other ILPs. Thus, our work demonstrates that onset of oogenesis and fertilization are subject to different ILP signals and sensory neuron activities, which ensure optimal reproduction within a changing environment.

Results

The bacterial food source modulates onset of oogenesis and fertilization rate in *C. elegans*

Previously, we have shown that different *E. coli* strains that serve as food for *C. elegans* can modulate the animals' reproductive physiology, independent of their somatic development (***Maier et al., 2010***). Wild-type *C. elegans* fed two different *E. coli* strains, OP50 and CS180, developed through four larval stages (L1 to L4; ***Figure 1A***) at about the same rate ($p = 0.72$; ***Figure 1B***), before they molted into young adults. However, *C. elegans* grown on CS180 produced less progeny when compared to animals grown on OP50 (***Figure 1C***, ***Figure 1—supplement 1***). This CS180-dependent phenotype was not

because the animals had restricted food intake, since they showed no delay in developmental rates (***Figure 1B***). In fact, CS180-fed animals exhibited faster fertilization rates during the first 24 hours of adulthood (***Figure 1D***, ***Figure 1—supplement 1***), which is opposite of what would be expected for food level-restricted animals (***Maier et al., 2010***).

In *C. elegans*, the total number of sperm made before the gametogenesis switch to oogenesis can limit the number of progeny (***Ward and Carrel, 1979***). Consistent with this idea, animals fed CS180 not only had fewer progeny (***Figure 1C***, ***Figure 1—supplement 1***), but also fewer sperm than animals on OP50 (***Figure 1E***). To test the hypothesis that the lower sperm number in *C. elegans* on CS180 was because of an earlier switch from spermatogenesis to oogenesis, we examined when the oogenesis marker *lin-41::GFP* (***Spike et al., 2014; Noble et al., 2016***) was first expressed (***Figure 1F and G***). We found that a significant fraction of worms on CS180 began to express the oogenesis marker at the mid-L4 stage, which was before the marker was observed in any worms on OP50 (***Figure 1H***, ***Figure 1—supplement 1***). Worms fed OP50 started to express *lin-41::GFP* only at late L4 (34%), when most animals on CS180 (69%) had already expressed the GFP marker (***Figure 1H***, ***Figure 1—supplement 1***). The gonads of CS180-fed animals also had more arrested oocytes than the gonads of age-matched adults on OP50 (***Figure 1I***). Thus, our data show that the fewer progeny on CS180 is a readout for earlier oogenesis on this food source. Together with the increased rate of fertilization in CS180-fed animals (***Figure 1D***, ***Figure 1—supplement 1***), which would depend on the oocyte maturation rate (***McCarter et al., 1999***), our data suggest that CS180 promotes earlier and faster oocyte development.

Food-type effects on oocyte development are independent of bacterial LPS structure

OP50 is derived from an *E. coli* B strain (***Brenner, 1974***); CS180, from an *E. coli* K-12 strain (***Pradel et al., 1992***). One of the well-characterized differences between the two bacterial strains is the outer core structures of the lipopolysaccharides (LPS) on their cell walls [(***Maier et al., 2010***) and references therein]. The OP50 LPS is shorter than the CS180 LPS [***Figure 2A***; (***Maier et al., 2010***)]. To test if this difference in LPS alters oogenesis onset and fertilization rate, we examined wild-type *C. elegans* oocyte development on *E. coli* CS2429, which is a K-12 strain that is derived from CS180 but has a truncated LPS [***Figure 2A***; (***Pradel et al., 1992; Zhang et al., 2006***)]. Interestingly, like on CS180, worms on CS2429 still displayed a lower number of progeny (***Figure 2B, Figure 2—supplement 1***), an early onset of oogenesis (***Figure 2C, Figure 2—supplement 1***), and faster fertilization (***Figure 2D, Figure 2—supplement 1***). This indicates that this difference in LPS structure is insufficient to affect oocyte development.

Although an alteration in LPS structure failed to elicit an oogenic response, it remains possible that the differences between OP50 and CS180 stimulate *C. elegans* innate immunity, which in turn modulate oocyte fate and physiology. Thus, we exposed the worms to two strains of the more pathogenic *Serratia marcescens* (***Pradel et al., 2007***) and again observed no early onset in oogenesis (***Figure 2E, Figure 2—supplement 1***). These findings suggest that these food-type responses are not general innate immune responses and also show that bacterial pathogenicity is insufficient to promote an early onset in oogenesis or faster fertilization.

Food type modulates oogenesis onset and fertilization rate at different critical periods during development

To identify the critical periods for food type-dependent effects on onset of oogenesis and on fertilization, we grew worms on one food type and switched them to the second food type at different stages of larval development. Worms that were switched from OP50 to

CS180 at the first larval stage (L1; ***Figure 3—supplement 1***) and at the early part of the third larval stage (L3) behaved like worms that were fed CS180 continuously (***Figure 3A and B, Figure 3—supplement 1***). These worms produced less progeny (***Figure 3A, Figure 3—supplement 1***) and expressed the oogenesis reporter earlier than animals grown continuously on OP50 (***Figure 3B, Figure 3—supplement 1***). Since the germ cells of worms transferred to CS180 still responded to this food source, this suggests that the germ cell decision to switch to oogenesis occurs after early L3.

In contrast, animals that were transferred from OP50 to CS180 at late L3 or later developmental stages showed the phenotype of animals that were always grown on OP50 (***Figure 3A and B, Figure 3—supplement 1***), which suggests that the germ cell decision to switch to oogenesis has already been made by late L3. This is further supported by our findings that the germ cells of worms that underwent the reciprocal switch from CS180 to OP50 responded consistently to OP50 only till early L3, but not at later stages (***Figure 3A and B, Figure 3—supplement 1***). Thus, food type can only modulate onset of oogenesis before late L3, consistent with a prior study that showed that germ cell fate determination occurs during this stage (***Barton and Kimble, 1990***).

However, the critical window for the food-type effect on fertilization rate is after the early part of the fourth larval stage (L4; ***Figure 3C to F, Figure 3—supplement 1***). Worms switched between one food source to the second food source at early L4 (***Figure 3D, Figure 3—supplement 1***) had the same fertilization rates as animals consistently fed the second food source. Animals switched at mid-L4 had a delayed and less robust fertilization response to the second food source (***Figure 3E, Figure 3—supplement 1***), whereas a food switch immediately after the molt into adulthood had no effect on fertilization rates (***Figure 3F, Figure 3—supplement 1***). Thus, fertilization rate is influenced by food type until just before *C. elegans* molts into a young adult.

A specific sensory neuron regulates the food-type differences in total progeny

We have previously shown that sensory perception of food type can alter *C. elegans* longevity (***Maier et al., 2010***), which led us to hypothesize that sensory neurons will also influence the number of progeny the animals produce on the different food sources. Accordingly, we tested mutants that impaired different subsets of sensory neurons. Unlike wild type, the *osm-3* mutant, which has many defective sensory neurons (***Tabish et al., 1995; Taylor et al., 2021***), produced the same number of offspring on both OP50 and CS180 (***Figure 4A, Figure 4—supplement 1***). This suggests that at least some of the *osm-3*-expressing neurons alter the worm's total progeny in response to food type.

Similar to *osm-3* mutants, a mutation in the guanylyl cyclase gene *odr-1*, which impairs a different subset of sensory neurons (***L'Etoile and Bargmann, 2000; Taylor et al., 2021***), also produced the same number of progeny on OP50 and CS180 (***Figure 4A, Figure 4—supplement 1***). However, unlike *osm-3* and *odr-1* mutants, but like wild type, a defect in the transcription factor gene *odr-7*, which causes the specific loss of the olfactory neuron AWA (***Sengupta et al., 1994***), led to more progeny on OP50 than on CS180 (***Figure 4A, Figure 4—supplement 1***). This suggests that there is some neuronal specificity in the regulation of this phenotype.

osm-3 and *odr-1* mutants share defects in several sensory neurons, including ASI, ASJ and ASK (***Tabish et al., 1995; L'Etoile and Bargmann, 2000; Taylor et al., 2021***). Individual ablation of the ASI and ASK neurons did not abolish the food type-dependent differences in total progeny (***Figure 4A, Figure 4—supplement 1***). Interestingly, loss of the ASJ neurons suppressed the differences in progeny number (***Figure 4A, Figure 4—supplement 1***) on OP50 versus CS180. Thus, our data show that, unlike ASI, ASK and AWA, the neuron ASJ modulates the worm's total progeny in response to food cues.

The ILP *ins-6* also regulates food-type differences in total progeny

The number of *C. elegans* progeny is also subject to regulation by insulin signaling [reviewed by (***Murphy and Hu, 2013***)], which led us to test whether insulin signaling will modulate the food-type differences in progeny number. Reduction-of-function mutations in *daf-2*, the *C. elegans* insulin-like growth factor receptor (***Kimura et al., 1997; Gems et al., 1998***), reduced or abolished the food-type differences in total progeny (***Figure 4B, Figure 4—supplement 1***). A loss-of-function mutation in *daf-16*, the FOXO-like transcriptional effector of insulin signaling (***Lin et al., 1997; Ogg et al., 1997***), also caused animals to decrease or eliminate the differences in their number of progeny on OP50 and CS180 (***Figure 4B and D, Figure 4—supplement 1***). Thus, the loss of food-type differences in these mutants indicates that insulin signaling regulates total progeny in response to food cues.

Because ASJ neurons express at least three potential ILP ligands for the DAF-2 receptor, INS-1 (***Kodama et al., 2006; Tomioka et al., 2006***), INS-6 (***Cornils et al., 2011***) and DAF-28 (***Li et al., 2003; Taylor et al., 2021***), we tested the effects of these three peptides on progeny number. Deletion of either *ins-1* or *daf-28* did not alter the OP50- or CS180-dependent progeny number (***Figure 4C, Figure 4—supplement 1***). However, *ins-6* deletion mutants lost the food-type differences in total progeny (***Figure 4D, Figure 4—supplement 1***), similar to *daf-16* mutants (***Figure 4D, Figure 4—supplement 1***). Together these data suggest that there are specific ILPs, such as INS-6, that modulate food type-dependent total progeny by acting through the insulin pathway effector DAF-16.

ASJ sensory neurons modulate the food type-dependent onset of oogenesis through INS-6

Since decreased progeny on CS180 reflects an earlier onset of oogenesis at mid-L4 (***Figure 1C and H, Figure 1—supplement 1***), we next asked whether ASJ is also required

to promote oogenesis in response to food-derived cues. For comparison, we determined in parallel the onset of oogenesis in *osm-3* mutants and in animals lacking ASI neurons.

Consistent with the loss of food-type differences in its total progeny (***Figure 4A, Figure 4—supplement 1***), *osm-3* mutants failed to exhibit an early onset in oogenesis on CS180 during mid-L4 (***Figure 5A, Figure 5—supplement 1***), which suggests that there are *osm-3*-expressing neurons that promote early oogenesis in response to food cues. In contrast, worms lacking ASI neurons showed early oogenesis during mid-L4 (***Figure 5A, Figure 5—supplement 1***). Yet, the continued low level of oogenesis during late L4 in ASI-ablated worms on CS180 might suggest that ASI plays a minor role in oogenesis and that the food-type differences in total progeny can be uncoupled from the food-type differences in oogenesis onset. More importantly, ASJ-ablated worms showed no early oogenesis at mid-L4 and decreased oogenesis even during late L4 and lethargus (***Figure 5A, Figure 5—supplement 1***). Thus, these findings demonstrate that ASJ neurons not only modulate the animal's number of progeny, but also play a major role in promoting oogenesis onset.

How does ASJ promote oogenesis? Again, the ILPs expressed by ASJ are good candidates through which ASJ affects this process, since insulin signaling is an important regulator of oocyte development across metazoans [reviewed by (***Das and Arur, 2017***)]. Indeed, both *daf-2* reduction-of-function mutants lost the early expression of the oogenesis marker *lin-41::GFP* on CS180 (***Figure 5B, Figure 5—supplement 1***), which suggests that insulin signaling also mediates the food-type effects on worm oogenesis. To determine whether the same ILP that regulates total progeny again regulates early oogenesis onset, we assayed the effects of *ins-6* on oogenesis and compared these to the effects of *ins-1* and *daf-28*. Similar to their lack of effect on food type-dependent total progeny (***Figure 4C, Figure 4—supplement 1***), the deletion of *ins-1* or *daf-28* had no effect on the OP50- or CS180-dependent onset of oogenesis (***Figure 5C, Figure 5—supplement 1***). However, *ins-6* mutants had little to no early expression of *lin-41::GFP* at mid-L4 (***Figure***

5C and E, Figure 5—supplement 1), which can be rescued by driving *ins-6* expression from its own promoter (***Figure 5E, Figure 5—supplement 1***). Thus, our data show that of the 3 ILPs tested, *ins-6* alone is sufficient to modulate the food type-dependent onset of oogenesis and behaves like *daf-2* in this process (***Figure 5B, Figure 5—supplement 1***).

During the larval stages, *ins-6* is expressed in two sensory neurons, ASI and ASJ (***Cornils et al., 2011***). Using the *drcSi68* transcriptional reporter, which expresses *ins-6p::mCherry* in ASI and ASJ, we asked whether the *ins-6* reporter expression changes when the animals are fed OP50 versus CS180. At mid-to-late L3, the stage when food source can still modulate oogenesis onset (***Figure 3B, Figure 3—supplement 1***), worms grown on CS180 showed higher *ins-6p::mCherry* expression in ASJ, but not in ASI, unlike worms on OP50 (***Figure 5D***). When we drove *ins-6* expression specifically in ASI or ASJ, we found that ASJ-expressed *ins-6*, but not ASI-expressed *ins-6*, is sufficient to rescue the oogenesis onset phenotype of *ins-6* mutants (***Figure 5E, Figure 5—supplement 1***). These findings suggest that ASJ modulates onset of oogenesis by producing INS-6.

AWA olfactory neurons and insulin receptor signaling regulate food type-dependent fertilization rates through different mechanisms

Next, we asked if sensory neurons also influence fertilization. While the *odr-1* mutation had little effect on food type-dependent fertilization rates (***Figure 6—supplement 1***), a mutation in either *osm-3* or another sensory gene, the G protein α subunit *odr-3* (***Roayaie et al., 1998***), suppressed the faster fertilization on CS180 (***Figure 6A and B, Figure 6—supplement 1***). This again suggests a role for sensory neurons in the food type-dependent modulation of fertilization rates.

Both *osm-3* and *odr-3* are expressed in several chemosensory neurons, including ADF, ASH, ASI, ASK and ASJ (***Tabish et al., 1995; Roayaie et al., 1998; Taylor et al.,***

2021). Ablation of either ADF or ASH had no effect on the food type-induced variation in fertilization rates (***Figure 6C and D, Figure 6—supplement 1***). While the global fertilization rates were lower on OP50 and CS180, loss of either ASI or ASK again did not abolish the food-type differences in fertilization (***Figure 6E and F, Figure 6—supplement 1***). In addition, the ASJ neurons, which modulate onset of oogenesis (***Figure 5A, Figure 5—supplement 1***), did not affect fertilization rates on OP50 versus CS180 (***Figure 6G, Figure 6—supplement 1***), suggesting that ASJ specifically influences oogenesis, but not fertilization. Thus, our data suggest that other neurons expressing either *osm-3* and/or *odr-3*, either individually or in combination, will modulate food type-dependent fertilization.

We also asked if the *odr-3*-expressing olfactory neurons AWA, AWB and AWC (***Roayaie et al., 1998***) play a role in this process. While loss of AWB and AWC did not eliminate the fertilization rate differences on OP50 and CS180 (***Figure 6H and I, Figure 6—supplement 1***), loss of AWA (***Sengupta et al., 1994; Yoshida et al., 2012***) suppressed the food-type differences in fertilization (***Figure 6J, Figure 6—supplement 1***). However, this AWA-dependent regulation of fertilization is independent of the AWA-specific olfactory receptor ODR-10 [***Figure 6—supplement 1***; (***Sengupta et al., 1996***)]. This suggests that AWA neurons regulate fertilization in response to food cues that are not ligands of ODR-10.

Next, we asked if AWA and ASJ act synergistically during fertilization. However, we found no synergistic effect between the two neurons in regulating this process (compare ***Figure 6G and J to Figure 6K, Figure 6—supplement 1***). To determine if AWA neurons specifically regulate fertilization, we then examined when oogenesis begins in animals lacking AWA. We found that absence of AWA had no effect on early onset of oogenesis on CS180 (***Figure 6L, Figure 6—supplement 1***), similar to its lack of effect on progeny number (***Figure 4A, Figure 4—supplement 1***). Moreover, we observed no synergistic effect between AWA and ASJ in regulating oogenesis onset (***Figure 6L,***

Figure 6—supplement 1). Thus, on given diets, we show that there are specific neurons that influence distinct aspects of oocyte development and physiology: ASJ for oogenesis onset versus AWA for fertilization.

To explore whether AWA regulates fertilization through insulin signaling, we assayed the food type-dependent fertilization rates of insulin signaling mutants. The weak reduction-of-function mutant *daf-2*(*e1368)* or the null *daf-16* mutant had little or no significant effect on fertilization (***Figure 7A and C, Figure 7—supplement 1***), but the stronger reduction-of-function mutant *daf-2(e1370)* (***Lin et al., 1997; Gems et al., 1998***) suppressed global fertilization rates (***Figure 7B, Figure 7—supplement 1***). However, the *daf-2(e1370)* mutant fertilization rate on OP50 still differed from that on CS180 (***Figure 7B, Figure 7—supplement 1***). This suggests that the DAF-2 receptor modulates overall fertilization rates, but not necessarily in response to food-derived cues. For this reason, the AWA food type-dependent influence on fertilization differs from the effects of insulin receptor signaling on this process.

To test if the ILPs that regulate fertilization also differs from the ILPs that regulate total progeny or oogenesis onset, we measured the effects *of ins-6, daf-28* or *ins-1* on fertilization. A single deletion of any of these ILPs had no effect on fertilization rates (***Figure 7D to F, Figure 7—supplement 1***), whereas deletion mutant combinations of these ILPs (***Figure 7—supplement 1***) did not exhibit any robust phenotypes that mirrored those of the strong *daf-2(e1370)* mutant phenotypes. This implies that there are multiple ILPs that act through the DAF-2 receptor to regulate fertilization. Notably, our findings indicate that the set of ILP activities that regulates fertilization is distinct from the set of ILPs that regulates onset of oogenesis.

Discussion

Germline development must be coordinated with existing environmental resources to optmize population survival. The sensory system is an important interface between the environment and an animal's physiology, which suggests a role for the sensory system in germline physiology. Not surprisingly, sensory neurons have been implicated in germline proliferation or senescence in *C. elegans* (***Dalfo et al., 2012; Sowa et al., 2015; Aprison and Ruvinsky, 2017***) and potentially in gamete development in mammals (***Boehm et al., 2005; Yoon et al., 2005***). Here we show that distinct sensory neurons acting through insulin-dependent and -independent signaling mechanisms influence specific steps in oocyte development and physiology in response to food-derived cues. Thus, discrete stages of oocyte development are subject to different sets of cues that are sensed by different cells that work together to control reproduction.

The sensory neurons that regulate oogenesis onset differ from those that affect fertilization

Unlike the olfactory neuron AWA, the chemosensory neuron ASJ promotes early onset of oogenesis (***Figure 6L, Figure 6—supplement 1, Figure 8***). This ASJ-dependent effect does not appear to be a general response to stress, like pathogen stress (***Figure 2E, Figure 2—supplement 1***), but a response to specific food cues. In contrast, the olfactory neuron AWA promotes the increased fertilization rates on the CS180 food source, but not ASJ and the other neurons we have so far tested (***Figure 6A to K, Figure 6—supplement 1, Figure 8***). Together these data show that the sensory cues that influence oogenesis onset differ from the sensory cues that affect fertilization.

While AWA has a major role in food type-dependent fertilization, it is most likely not the only sensory neuron involved in this process. The *osm-3* mutation, which impairs several sensory neurons (***Tabish et al., 1995***), also partly suppresses the faster fertilization on CS180 (***Figure 6A, Figure 6—supplement 1***). This raises the likelihood

that other neurons regulate fertilization. In fact, we find that worms lacking ASI, ASK and AWB neurons fertilize at a slower rate at certain or at all time points on OP50 and CS180, when compared to wild type (***Figure 6E, F and H, Figure 6—supplement 1***). However, these animals still exhibit significant food-type differences in their fertilization rates (***Figure 6E, F and H, Figure 6—supplement 1***), which means that ASI, ASK and AWB are not required to regulate food-type effects on fertilization, but might have a role that are independent of food. A mechanism that includes several neurons to regulate fertilization would be expected, since it is a dynamic process that proceeds for several days. This makes it necessary for the worms to sense environmental changes continuously and adjust their reproductive physiology accordingly. Thus, the involvement of multiple sensory neurons would make for a more sensitive and efficient physiology.

Interestingly, at least one of the sensory neurons that inhibits germline proliferation (***Aprison and Ruvinsky, 2017***), ASJ, also promotes food type-dependent early oogenesis (this work). This suggests that this sensory neuron might regulate oogenesis onset by regulating the first switch that occurs in the *C. elegans* germline, mitosis (*i.e.*, proliferation) to meiosis (*i.e.*, differentiation) (***Kimble and Crittenden, 2007***). Consistent with this hypothesis, we demonstrate that food type can only modulate onset of oogenesis before the late L3 stage (***Figure 3B, Figure 3—supplement 1***), which coincides with the time before germ cells enter meiosis (***Kimble and Crittenden, 2007***). Thus, some of the sensory neurons that influence the germline might have more than one function at different stages of germ cell development.

Oocyte development requires distinct insulin-like signaling mechanisms

Insulin signaling is an important regulator of oogenesis, where impaired signaling leads to reproductive deficits across many species [reviewed by (***Das and Arur, 2017***)]. Here we find that specific ILPs regulate discrete stages of oocyte physiology. The ILP INS-6 acts

from the ASJ neuron to modulate food type-dependent onset of oogenesis (***Figure 5E, Figure 5—supplement 1, Figure 8***), whereas it appears to have little or no effect on oocyte fertilization rates (***Figure 7D, Figure 7—supplement 1***). Although insulin receptor DAF-2 signaling does not appear to mediate the AWA neuron-dependent food-type effects on fertilization, DAF-2 does regulate overall fertilization independent of food sources (***Figure 7B, Figure 7—supplement 1, Figure 8***), where its ILP ligands remain to be identified. Since fertilization depends on oocyte maturation (***McCarter et al., 1999***), our data also suggest that different ILPs regulate specific stages of oogenesis—onset versus maturation.

These ILPs might encode and integrate diverse environmental cues that influence oocyte development. Considering the pleiotropic effects of insulin signaling in metazoan reproduction (***Das and Arur, 2017***), it is possible that the multiple ILPs present in other animals (***Allen et al., 2015***) will also have distinct roles in coordinating oogenesis with fluctuations in a given environment. Thus, our study suggests that successful fertilization will require the careful integration of multiple environmental inputs through ILPs acting on the germline from neuronal, and potentially non-neuronal, cells.

Materials and Methods

General worm maintenance

C. elegans were cultured on NGM agar plates (***Brenner, 1974***) seeded with *E. coli* OP50, CS180, or CS2429 or with *S. marcescens* strains. All animals were well-fed for at least two generations before any phenotypic analyses were conducted. All experiments were performed at 25°C, except for those that included the *daf-2(e1368)* or *daf-2(e1370)* temperature-sensitive mutations. *daf-2* mutants grown as eggs until the L1 stage at 25°C become developmentally arrested (***Gems et al., 1998***). Thus, these mutants were first grown at 20°C, the permissive temperature, and shifted to 25°C before the critical periods

defined for food-dependent modulation of oogenesis onset or fertilization, along with their corresponding controls. See ***Supplementary File 1*** for the list of genotypes of the strains used in this study, which include the neuronally ablated animals.

Measurement of the rate of development

L1 larvae that hatched within a 2-hr period on each bacterial food source were collected and allowed to grow at 25°C for 32 hrs on the same food source. The number of animals that were L1, L2, L3 or L4 larvae or adults were counted and represented as a percentage of the total population. The chi-square test was used to compare the stage distributions of worms fed the different bacteria.

Measurement of sperm and arrested oocytes

To count the number of sperm, 2- to 3-hr-old adult OD95 hermaphrodites that carry the transgene *pie-1p::mCherry::his-58* (***McNally et al., 2006***) were anesthetized on a 1% agarose pad that contain 6 mM sodium azide. Series of Z-stack images of the spermathecae were captured at 100 msec as the exposure time, using a Nikon Eclipse Ti-E microscope and a Photometrics Coolsnap Myo cooled digital camera. The number of sperm were counted as red fluorescent puncta across the entire stacks.

To measure the number of arrested oocytes, young wild-type adult hermaphrodites were anesthetized as described above. The gonads were imaged under differential interference contrast microscopy. Counts from only one gonad arm were reported per animal. The Student's t-test was used to compare gamete counts between animals.

Measurement of total progeny

Individual young adult hermaphrodites were grown on a 35-mm plate seeded with the indicated bacteria. The mother was transferred to a new plate every 12-24 hrs until

reproduction ceased entirely. Total progeny that hatched were counted and reported. At least ten animals were tested in each trial, and each strain studied was assayed in multiple independent trials. To analyze the *daf-2* mutants and their corresponding controls, worms were first grown at 20°C, before they were transferred to 25°C at the early L3 stage. Statistical comparisons across multiple groups were determined by one-way ANOVA, followed by Tukey's correction.

Imaging the oogenesis reporter

Control and mutants carrying the *lin-41::GFP* reporter (***Spike et al., 2014***) were imaged at 400X magnification, using the Nikon Eclipse Ti-E microscope and a Photometrics Coolsnap Myo cooled digital camera. The exposure time was set at 500 msec, and the presence or absence of GFP was reported at different stages. The stages of the animal were determined by observing the vulval morphology under 400x, as described by (***Mok et al., 2015***), and illustrated in ***Figure 1F***. Based on the substages described by ***Mok et al.*** (***2015***), early L4 corresponded to the L4.0 to L4.2 substages; mid L4, to the L4.3 to L4.5 substages; late L4, to the L4.6 to L4.8 substages, when the finger-like structures that formed at the sides of the vulva (red arrowheads in ***Figure 1F***) had started to migrate ventrally; and lethargus to the L4.9 substage. To analyze the *daf-2* mutants and their corresponding controls, worms were grown at 20°C and transferred to 25°C at the early L3 stage and then imaged at different subsequent stages. Statistical comparisons across multiple groups used the Fisher's exact test.

Imaging the *ins-6p::mCherry* transcriptional reporter

Generation of the ins-6p::mCherry transcriptional reporter. The mCherry gene was flanked with 1.64-kb sequences upstream of the *ins-6* start codon and 7.57-kb sequences downstream of the *ins-6* stop codon. This reporter was cloned into a MosSCI vector for

integration (pQL147) at the ttTi5605 site of chromosome II (***Frøkjær-Jensen et al., 2008***) to generate the *ins-6p::mCherry drcSi68* worms.

Imaging of drcSi68 worms. The worms were grown continuously on OP50 or CS180. Worms at the mid-to-late L3 stage were imaged at 1000x magnification, using a Nikon Eclipse Ni-U microscope and a Photometrics Coolsnap ES2 cooled digital camera. The exposure time was set at 50 msec. Fluorescence intensities were quantified using a built-in fluorescence quantification algorithm (NIS-Elements, Nikon Instruments, Inc). Statistical analyses used two-way ANOVA and Tukey's correction.

Measuring the rates of fertilization

For every trial, ten to twelve young adult worms were grown singly for a specified number of hours. At the end of each time point, the mother was bleached in a 5% sodium hypochlorite solution to release and count the fertilized embryos within its uterus. We also counted the number of hatched progeny that were laid on the plates. The total number of oocytes fertilized at each time point was the sum of the embryos within the uterus and those laid on the plates. We then divided the total number of fertilized oocytes by the duration of the collection to calculate the rate of fertilization at that specific time point. To analyze the *daf-2* mutants and their corresponding controls, worms were first grown at 20°C and transferred to 25°C at the early L4 stage. Statistical comparisons across multiple groups were performed by two-way ANOVA and Tukey's correction.

To compare the food type-dependent changes in fertilization rates between wild type and different groups of animals, we normalized the 12- to 24-hour fertilization rates on CS180 to the 12- to 24-hour fertilization rates on OP50 of a given strain. The resulting normalized means were then compared to the food type-dependent change in fertilization rates of wild-type controls. Thus, p values were calculated by obtaining the t-score after

comparing the % change in wild type on CS180 versus OP50 to the % change for the specific mutant on CS180 versus OP50.

Food-switch experiments

C. elegans were grown on each bacteria and then transferred to the second bacteria at different stages. The early L3, late L3, early L4, and late L4 were determined based on the developmental rates of the animals on OP50 and CS180. L1 larvae that hatched within a 1-hr period at 25°C were collected and allowed to develop further at this temperature on the first bacteria for a certain duration before being shifted to the second bacteria: 20 hrs for early L3, 24 hrs for late L3, and 26 and 30 hrs, respectively, for early and late L4. The early and late L4 stages were also confirmed by examining vulval morphology. To minimize contamination from the earlier bacteria, worms were allowed to roam on the second bacteria for 45-60 minutes and then transferred to a fresh plate seeded with the second bacteria. After this transfer, worms were assayed for total number of progeny, fertilization rate, or the expression of the *lin-41::GFP* reporter.

To compare the food type-dependent changes in fertilization rates during the food switches, we normalized the 12- to 24-hour fertilization rates of the CS180-to-OP50 switched animals to the 12- to 24-hour fertilization rates of the OP50-to-CS180 switched animals. The p values of the subsequent normalized means were calculated by obtaining the t-score after comparing the % change in food-switched animals to the % change in non-switched controls on CS180.

Statistical analysis

Statistical analyses were done using GraphPad Prism 8 software. For more details, refer to above and the legends of the figures and their supplements.

Acknowledgements

We thank S. Mitani, the *Caenorhabditis* Genetics Center (funded by NIH P40 OD010440), J. Apfeld, T. Chen, D. Ferkey, M. Goodman, J. Klena, and P. Sengupta for strains used in this study. We also thank S. Kuchin of University of Wisconsin-Milwaukee for generously assisting us in the statistical analyses of total fertilization rates of different worm genotypes on different food sources (***Figures 3, 6 and 7 Supplements, sheets on normalized fertilization rates***). We further thank A. Shevade and M. Salsaa for comments on the manuscript. This work was supported by a Wayne State University Graduate Research Assistantship to S. M., an ERC Starting Investigator Grant (NeuroAge 242666) and a Research Councils UK Fellowship to Q. C., and by Wayne State University, the Alcedo family and NIH (R01 GM108962) to J. A.

References

Allen E, Ren J, Zhang Y and Alcedo J. 2015. Sensory systems: their impact on *C. elegans* survival, *Neuroscience* **296**: 15-25.

Aprison EZ and Ruvinsky I. 2017. Counteracting ascarosides act through distinct neurons to determine the sexual identity of *C. elegans* pheromones, *Curr Biol* **27**: 2589-2599.

Barton MK and Kimble J. 1990. *fog-1*, a regulatory gene required for specification of spermatogenesis in the germ line of *Caenorhabditis elegans*, *Genetics* **125**: 29-39.

Boehm U, Zou Z and Buck LB. 2005. Feedback loops link odor and pheromone signaling with reproduction, *Cell* **123**: 683-95.

Brenner S. 1974. The genetics of *Caenorhabditis elegans*, *Genetics* **77**: 71-94.

Chen Z, Hendricks M, Cornils A, Maier W, Alcedo J and Zhang Y. 2013. Two insulin-like peptides antagonistically regulate aversive olfactory learning in *C. elegans*, *Neuron* **77**: 572-85.

Cornils A, Gloeck M, Chen Z, Zhang Y and Alcedo J. 2011. Specific insulin-like peptides encode sensory information to regulate distinct developmental processes, *Development* **138**: 1183-93.

Dalfo D, Michaelson D and Hubbard EJ. 2012. Sensory regulation of the *C. elegans* germline through TGF-beta-dependent signaling in the niche, *Curr Biol* **22**: 712-9.

Das D and Arur S. 2017. Conserved insulin signaling in the regulation of oocyte growth, development, and maturation, *Mol Reprod Dev* **84**: 444-459.

Duret L, Guex N, Peitsch MC and Bairoch A. 1998. New insulin-like proteins with atypical disulfide bond pattern characterized in *Caenorhabditis elegans* by comparative sequence analysis and homology modeling, *Genome Res* **8**: 348-53.

Fernandes de Abreu DA, Caballero A, Fardel P, Stroustrup N, Chen Z, Lee K, Keyes WD, Nash ZM, Lopez-Moyado IF, Vaggi F et al. 2014. An insulin-to-insulin regulatory network orchestrates phenotypic specificity in development and physiology, *PLoS Genet* **10**: e1004225.

Frøkjær-Jensen C, Wayne Davis M, Hopkins CE, Newman BJ, Thummel JM, Olesen S-P, Grunnet M and Jorgensen EM. 2008. Single-copy insertion of transgenes in *Caenorhabditis elegans*, *Nat Genet* **40**: 1375-1383.

Gems D, Sutton AJ, Sundermeyer ML, Albert PS, King KV, Edgley ML, Larsen PL and Riddle DL. 1998. Two pleiotropic classes of *daf-2* mutation affect larval arrest, adult behavior, reproduction and longevity in *Caenorhabditis elegans*, *Genetics* **150**: 129-55.

Greenstein D (2005) Control of oocyte meiotic maturation and fertilization. in The C. elegans Research Community (ed.) *WormBook*: WormBook.

Kawano T, Ito Y, Ishiguro M, Takuwa K, Nakajima T and Kimura Y. 2000. Molecular cloning and characterization of a new insulin/IGF-like peptide of the nematode *Caenorhabditis elegans*, *Biochem Biophys Res Commun* **273**: 431-6.

Kimble J and Crittenden SL. 2007. Controls of germline stem cells, entry into meiosis, and the sperm/oocyte decision in *Caenorhabditis elegans*, *Annu Rev Cell Dev Biol* **23**: 405-433.

Kimura KD, Tissenbaum HA, Liu Y and Ruvkun G. 1997. *daf-2*, an insulin receptor-like gene that regulates longevity and diapause in *Caenorhabditis elegans*, *Science* **277**: 942-6.

Kodama E, Kuhara A, Mohri-Shiomi A, Kimura KD, Okumura M, Tomioka M, Iino Y and Mori I. 2006. Insulin-like signaling and the neural circuit for integrative behavior in *C. elegans*, *Genes Dev* **20**: 2955–2960.

L'Etoile ND and Bargmann CI. 2000. Olfaction and odor discrimination are mediated by the *C. elegans* guanylyl cyclase ODR-1, *Neuron* **25**: 575-86.

Li W, Kennedy SG and Ruvkun G. 2003. *daf-28* encodes a *C. elegans* insulin superfamily member that is regulated by environmental cues and acts in the DAF-2 signaling pathway, *Genes Dev* **17**: 844-58.

Lin K, Dorman JB, Rodan A and Kenyon C. 1997. *daf-16*: An HNF-3/forkhead family member that can function to double the life-span of *Caenorhabditis elegans*, *Science* **278**: 1319–1322.

Maier W, Adilov B, Regenass M and Alcedo J. 2010. A neuromedin U receptor acts with the sensory system to modulate food type-dependent effects on *C. elegans* lifespan, *PLoS Biol* **8**: e1000376.

McCarter J, Bartlett B, Dang T and Schedl T. 1999. On the control of oocyte meiotic maturation and ovulation in *Caenorhabditis elegans*, *Dev Biol* **205**: 111-28.

McNally K, Audhya A, Oegema K and McNally FJ. 2006. Katanin controls mitotic and meiotic spindle length, *J Cell Biol* **175**: 881-891.

Michaelson D, Korta DZ, Capua Y and Hubbard EJ. 2010. Insulin signaling promotes germline proliferation in *C. elegans*, *Development* **137**: 671-80.

Miller MA, Nguyen VQ, Lee MH, Kosinski M, Schedl T, Caprioli RM and Greenstein D. 2001. A sperm cytoskeletal protein that signals oocyte meiotic maturation and ovulation, *Science* **291**: 2144-7.

Mok DZ, Sternberg PW and Inoue T. 2015. Morphologically defined sub-stages of *C. elegans* vulval development in the fourth larval stage, *BMC Dev Biol* **15**: 26.

Murphy CT and Hu PJ. 2013. Insulin/insulin-like growth factor signaling in C. elegans, *WormBook*: 1-43.

Noble DC, Aoki ST, Ortiz MA, Kim KW, Verheyden JM and Kimble J. 2016. Genomic analyses of sperm fate regulator targets reveal a common set of oogenic mRNAs in *Caenorhabditis elegans*, *Genetics* **202**: 221-34.

Ogg S, Paradis S, Gottlieb S, Patterson GI, Lee L, Tissenbaum HA and Ruvkun G. 1997. The Fork head transcription factor DAF-16 transduces insulin-like metabolic and longevity signals in *C. elegans*, *Nature* **389**: 994-9.

Perez MF, Shamalnasab M, Mata-Cabana A, Della Valle S, Olmedo M, Francesconi M and Lehner B. 2021. Neuronal perception of the social environment generates an inherited memory that controls the development and generation time of *C. elegans*, *Curr Biol* **31**: 1 - 13.

Pierce SB, Costa M, Wisotzkey R, Devadhar S, Homburger SA, Buchman AR, Ferguson KC, Heller J, Platt DM, Pasquinelli AA et al. 2001. Regulation of DAF-2 receptor signaling by human insulin and *ins-1*, a member of the unusually large and diverse *C. elegans* insulin gene family, *Genes Dev* **15**: 672-86.

Pradel E, Parker CT and Schnaitman CA. 1992. Structures of the rfaB, rfaI, rfaJ, and rfaS genes of Escherichia coli K-12 and their roles in assembly of the lipopolysaccharide core, *J Bacteriol* **174**: 4736-45.

Pradel E, Zhang Y, Pujol N, Matsuyama T, Bargmann CI and Ewbank JJ. 2007. Detection and avoidance of a natural product from the pathogenic bacterium *Serratia marcescens* by *Caenorhabditis elegans*, *Proc Natl Acad Sci USA* **104**: 2295-2300.

Ritter AD, Shen Y, Fuxman Bass J, Jeyaraj S, Deplancke B, Mukhopadhyay A, Xu J, Driscoll M, Tissenbaum HA and Walhout AJM. 2013. Complex expression dynamics and robustness in *C. elegans* insulin networks, *Genome Research* **23**: 954-965.

Roayaie K, Crump JG, Sagasti A and Bargmann CI. 1998. The G alpha protein ODR-3 mediates olfactory and nociceptive function and controls cilium morphogenesis in *C. elegans* olfactory neurons, *Neuron* **20**: 55-67.

Sengupta P, Chou JH and Bargmann CI. 1996. *odr-10* encodes a seven transmembrane domain olfactory receptor required for responses to the odorant diacetyl, *Cell* **84**: 899-909.

Sengupta P, Colbert HA and Bargmann CI. 1994. The *C. elegans* gene *odr-7* encodes an olfactory-specific member of the nuclear receptor superfamily, *Cell* **79**: 971-80.

Sowa JN, Mutlu AS, Xia F and Wang MC. 2015. Olfaction modulates reproductive plasticity through neuroendocrine signaling in *Caenorhabditis elegans*, *Curr Biol* **25**: 2284-9.

Spike CA, Coetzee D, Eichten C, Wang X, Hansen D and Greenstein D. 2014. The TRIM-NHL protein LIN-41 and the OMA RNA-binding proteins antagonistically control the prophase-to-metaphase transition and growth of *Caenorhabditis elegans* oocytes, *Genetics* **198**: 1535-58.

Tabish M, Siddiqui ZK, Nishikawa K and Siddiqui SS. 1995. Exclusive expression of *C. elegans osm-3* kinesin gene in chemosensory neurons open to the external environment, *J Mol Biol* **247**: 377-89.

Taylor SR, Santpere G, Weinreb A, Barrett A, Reilly MB, Xu C, Varol E, Oikonomou P, Glenwinkel L, McWhirter R et al. 2021. Molecular topography of an entire nervous system, *Cell* **184**: 4329-4347.e23.

Tomioka M, Adachi T, Suzuki H, Kunitomo H, Schafer WR and Iino Y. 2006. The insulin/PI 3-kinase pathway regulates salt chemotaxis learning in *Caenorhabditis elegans*, *Neuron* **51**: 613-25.

Ward S and Carrel JS. 1979. Fertilization and sperm competition in the nematode *Caenorhabditis elegans*, *Dev Biol* **73**: 304-21.

Yoon H, Enquist LW and Dulac C. 2005. Olfactory inputs to hypothalamic neurons controlling reproduction and fertility, *Cell* **123**: 669-82.

Yoshida K, Hirotsu T, Tagawa T, Oda S, Wakabayashi T, Iino Y and Ishihara T. 2012. Odour concentration-dependent olfactory preference change in *C. elegans*, *Nat Commun* **3**: 739.

Zhang P, Snyder S, Feng P, Azadi P, Zhang S, Bulgheresi S, Sanderson KE, He J, Klena J and Chen T. 2006. Role of N-acetylglucosamine within core lipopolysaccharide of several species of gram-negative bacteria in targeting the DC-SIGN (CD209), *J Immunol* **177**: 4002-11.

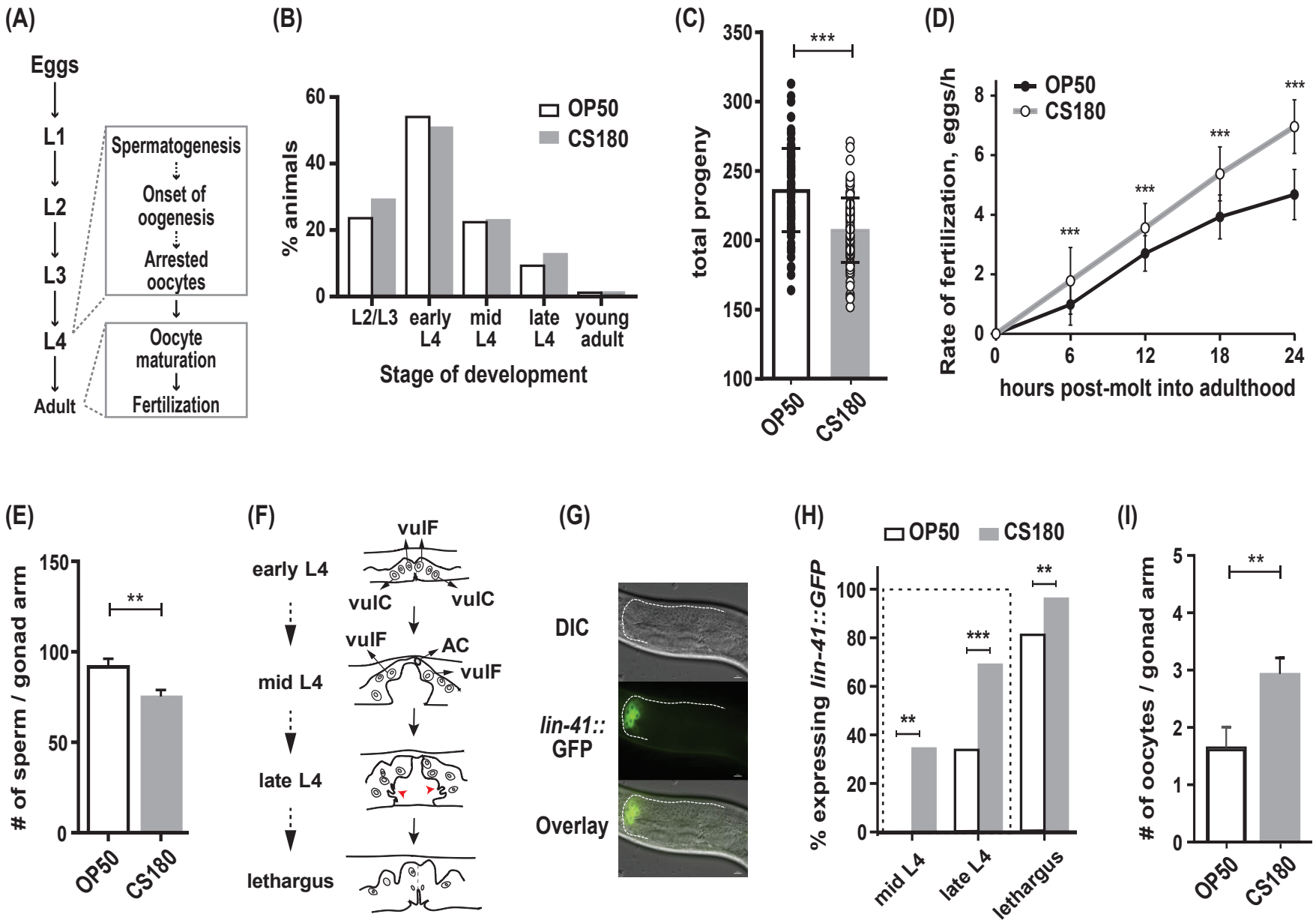
(A)
Eggs
L1
L2
L3
L4
Adult
Spermatogenesis
Onset of oogenesis
Arrested oocytes
Oocyte maturation
Fertilization
(B)
% animals
OP50
CS180
L2/L3
early L4
mid L4
late L4
young adult
Stage of development
(C)
total progeny
***
OP50
CS180
(D)
Rate of fertilization, eggs/h
OP50
CS180
hours post-molt into adulthood
(E)
# of sperm / gonad arm
**
OP50
CS180
(F)
early L4
mid L4
late L4
lethargus
vulF
vulC
AC
(G)
DIC
lin-41::GFP
Overlay
(H)
OP50
CS180
% expressing lin-41::GFP
mid L4
late L4
lethargus
(I)
# of oocytes / gonad arm
**
OP50
CS180

Figure 1. *C. elegans* exhibit early onset of oogenesis and faster fertilization rate in response to a specific bacterial food source. (A) The *C. elegans* reproductive developmental program, which depicts the timing of the spermatogenesis-to-oogenesis switch at L4. **(B)** Somatic development was unchanged between animals fed the two *E. coli* food types (n = 286 on OP50; n = 265 on CS180; p = 0.72). **(C-E)** Worms fed OP50 had more progeny (**C**), slower fertilization rates **(D)**, and more sperm **(E)** than worms fed CS180. **(F)** Simplified illustration of vulval morphology at various sub-stages of L4, where the nuclei of specific cells are shown [adapted from (***Mok et al., 2015***)]. Red arrowheads indicate the finger-like structures at the sides of the vulva, which migrate ventrally during late L4. Lethargus is the molting period from L4 to young adulthood. **(G)** Onset of oogenesis was determined by the initial expression of *lin-41::GFP*. Anterior is to the left and dorsal is to the top of each panel. Scale bar is 10 μm. **(H)** Worms on CS180 began oogenesis earlier at mid L4 than worms on OP50, based on the earliest *lin-41::GFP* expression. **(I)** Adults on CS180 also had more arrested oocytes than age-matched adults on OP50. Error bars in **(C-D)** represent standard deviation; (**E**, **I**), SEM. ** indicates $p \leq 0.01$; and ***, $p \leq 0.001$.

Figure 1—supplement 1. Statistical analyses of wild-type progeny, fertilization rates and oogenesis onset on OP50 versus CS180. Sheet 1 shows the analyses for total progeny; sheet 2, for fertilization rates; and sheet 3, for onset of oogenesis. On sheets 1 and 2, N is the total number of animals that were assayed. Means are from pooled data from multiple, independent trials. SD is the standard deviation. On sheet 3, GFP (+) and GFP (-) are animals that expressed or did not express the *lin-41::GFP* oogenesis marker, respectively. On all sheets, significant p values are shown in red and italicized. The figure panels associated with the data are indicated. * denotes p values between OP50-fed worms versus CS180-fed worms.

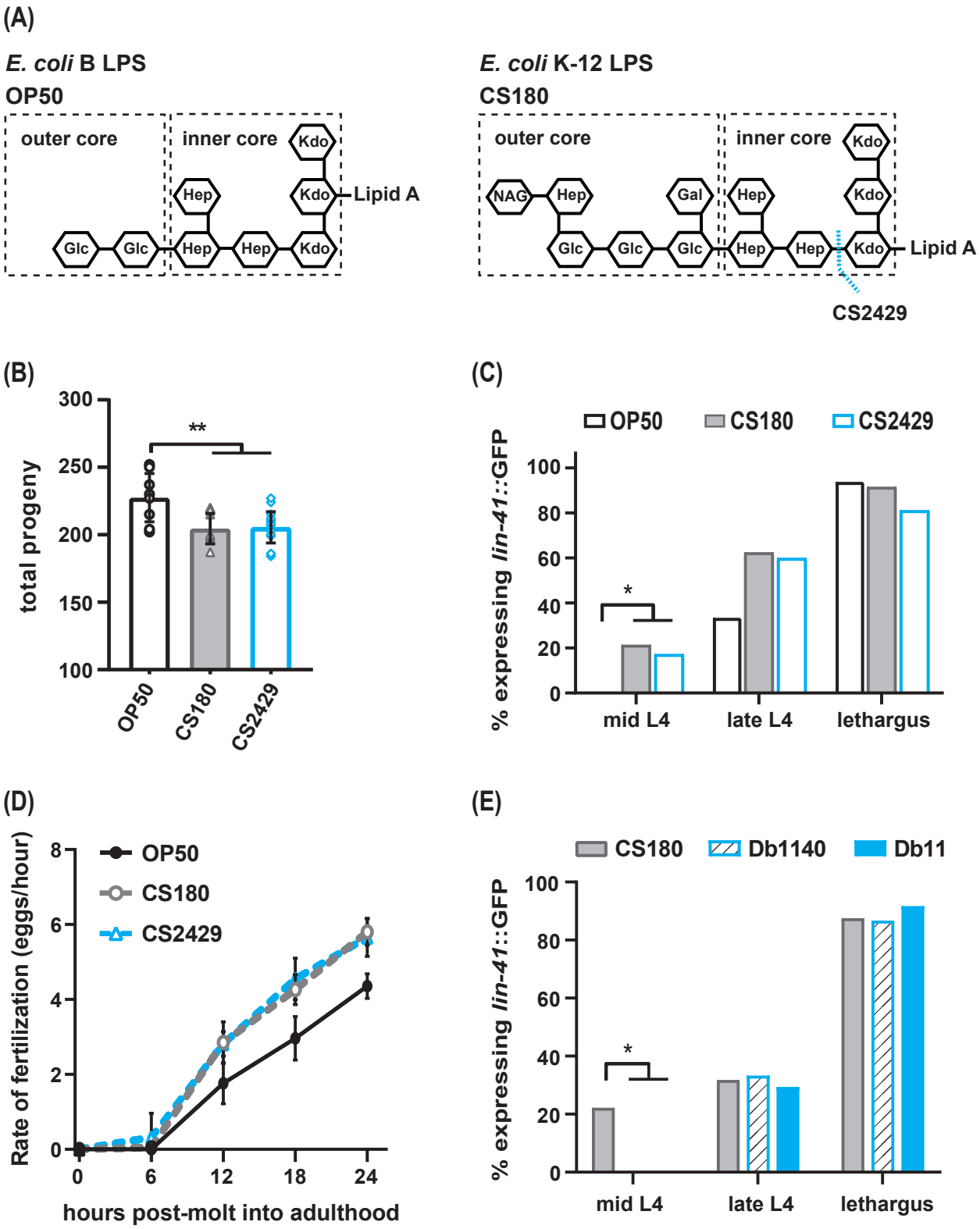
(A)
E. coli B LPS
OP50
outer core
inner core
Kdo
Hep
Kdo
Lipid A
Glc
Glc
Hep
Hep
Kdo
E. coli K-12 LPS
CS180
outer core
inner core
Kdo
NAG
Hep
Gal
Hep
Kdo
Glc
Glc
Glc
Hep
Hep
Kdo
Lipid A
CS2429
(B)
total progeny
300
250
200
150
100
**
OP50
CS180
CS2429
(C)
OP50
CS180
CS2429
% expressing lin-41::GFP
100
80
60
40
20
0
*
mid L4
late L4
lethargus
(D)
Rate of fertilization (eggs/hour)
8
6
4
2
0
OP50
CS180
CS2429
0
6
12
18
24
hours post-molt into adulthood
(E)
CS180
Db1140
Db11
% expressing lin-41::GFP
100
80
60
40
20
0
*
mid L4
late L4
lethargus

Figure 2. The food-type effects on oogenesis are independent of *E. coli* LPS length and general pathogenicity. (A) The LPS of *E. coli* B and K-12 strains. CS2429 is derived from CS180 and has a truncated LPS (***Maier et al., 2010***, and references therein). The dotted blue line indicates the site of truncation. **(B-D)** The shorter LPS of CS2429 elicited the same total progeny **(B)**, a similar pattern of oogenesis reporter expression **(C)**, and the same rate of fertilization **(D)**, as the longer LPS of the parent strain CS180. **(E)** Two strains of the pathogen *Serratia marcescens*, Db1140 and Db11, did not induce early oogenesis onset. Error bars represent standard deviations. * indicates $p \leq 0.05$; and **, $p \leq 0.01$.

Figure 2—supplement 1. Statistical analyses of wild-type progeny, oogenesis onset and fertilization rates on OP50, LPS mutant bacteria, and *Serratia marcescens*. Sheet 1 shows the analyses for total progeny; sheet 2, for onset of oogenesis; and sheet 3, for fertilization rates. On sheets 1 and 3, N is the total number of animals that were assayed. Means are from pooled data from multiple, independent trials. SD is the standard deviation. On sheet 2, GFP (+) and GFP (-) are animals that expressed or did not express the *lin-41::GFP* oogenesis marker, respectively. On all sheets, significant p values are shown in red and italicized. The figure panels associated with the data are indicated. NA means not applicable.

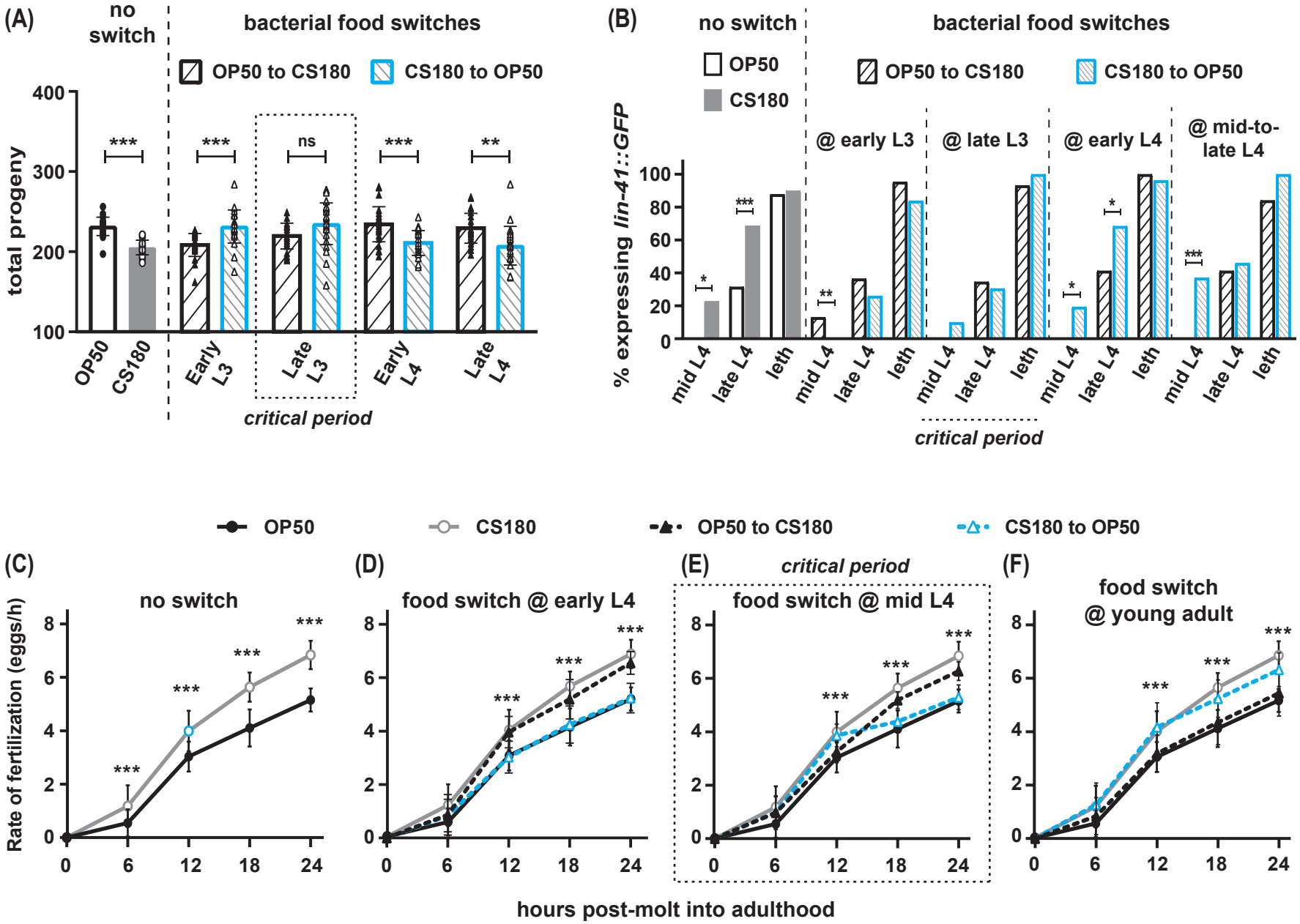
(A)
no switch
bacterial food switches
OP50 to CS180
CS180 to OP50
total progeny
400
300
200
100
***
***
ns
***
**
OP50
CS180
Early L3
Late L3
Early L4
Late L4
critical period
(B)
no switch
bacterial food switches
OP50
CS180
OP50 to CS180
CS180 to OP50
% expressing lin-41::GFP
@ early L3
@ late L3
@ early L4
@ mid-to-late L4
mid L4
late L4
leth
critical period
OP50
CS180
OP50 to CS180
CS180 to OP50
(C)
no switch
(D)
food switch @ early L4
(E)
critical period
food switch @ mid L4
(F)
food switch @ young adult
Rate of fertilization (eggs/h)
hours post-molt into adulthood

Figure 3. Food type modulates oogenesis onset during L3 and fertilization rates after early L4. *C. elegans* were shifted between *E. coli* OP50 and CS180 at different stages of larval development. **(A-B)** The critical period for food-type modulation of total progeny **(A)** and oogenesis onset **(B)** is around late L3. **(C-F)** The critical period for modulation of fertilization is after early L4. Error bars represent standard deviations. * indicates $p \leq 0.05$; **, $p \leq 0.01$; ***, $p \leq 0.001$; ns, not significant; and leth, lethargus.

Figure 3—supplement 1. Statistical analyses of the progeny, oogenesis onset and fertilization rates in food-switched versus non-switched wild-type animals. Sheet 1 shows the analyses for total progeny; sheet 2, for onset of oogenesis; sheet 3, for fertilization rates before normalization; and sheet 4, for normalized fertilization rates. On sheets 1 and 3, N is the total number of animals that were assayed. Means are from pooled data from multiple, independent trials. SD is the standard deviation. On sheet 2, GFP (+) and GFP (-) are animals that expressed or did not express the *lin-41::GFP* oogenesis marker, respectively. On all sheets, significant p values are shown in red and italicized. The figure panels associated with the data are indicated. Symbols, abbreviations and superscripted letters are described within each sheet.

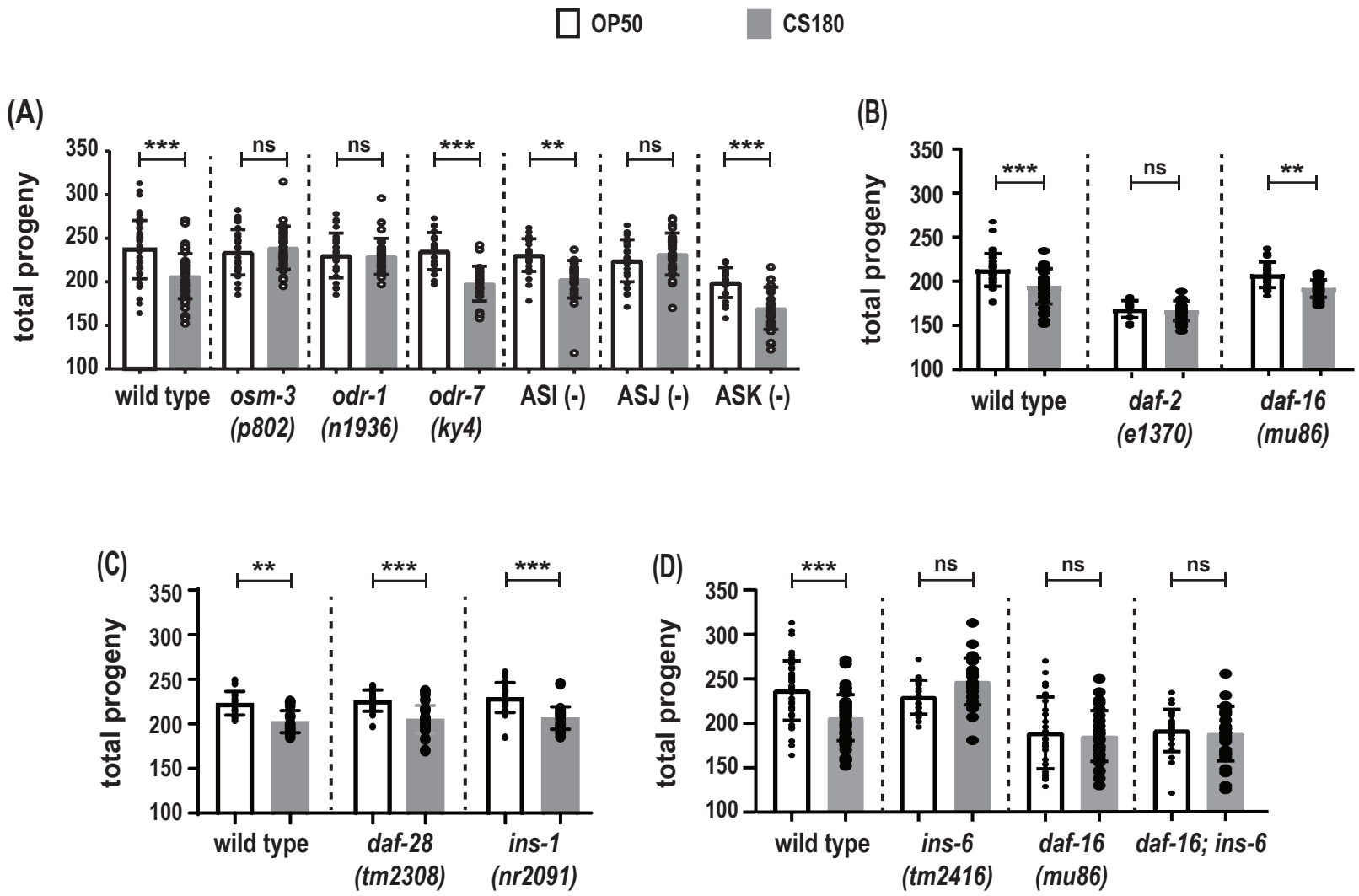
OP50
CS180
(A)
total progeny
350
300
250
200
150
100
***
ns
ns
***
**
ns
***
wild type
osm-3 (p802)
odr-1 (n1936)
odr-7 (ky4)
ASI (-)
ASJ (-)
ASK (-)
(B)
total progeny
***
ns
**
wild type
daf-2 (e1370)
daf-16 (mu86)
(C)
total progeny
**
***
***
wild type
daf-28 (tm2308)
ins-1 (nr2091)
(D)
total progeny
***
ns
ns
ns
wild type
ins-6 (tm2416)
daf-16 (mu86)
daf-16; ins-6

Figure 4. The ASJ sensory neuron and insulin-like peptide INS-6 alter total progeny in response to food type. **(A)** Food-type differences in total progeny were lost in sensory mutants *osm-3* and *odr-1* and in animals lacking the ASJ neurons. **(B)** Total progeny of the strong reduction-of-function mutant *daf-2(e1370)* and the *daf-16* loss-of-function mutant on OP50 and CS180. **(C-D)** OP50- and CS180-dependent progeny of ILP deletion mutants. Error bars represent standard deviations. ** indicates $p \leq 0.01$; ***, $p \leq 0.001$; and ns, not significant.

Figure 4—supplement 1. Statistical analyses of total progeny of different groups of animals on OP50 versus CS180. N is the total number of animals that were assayed. Means are from pooled data from multiple, independent trials. SD is the standard deviation. Significant p values are shown in red and italicized. The figure panels associated with the data are indicated. * denotes p values between OP50-fed worms versus CS180-fed worms. # denotes experiments in which animals that carry the *daf-2(e1368)*, *daf-2(e1370)*, or *daf-16(mu86)* mutation and the corresponding wild-type controls were grown at 20°C and transferred to 25°C at the early L3 stage. All other experiments involved animals that were continuously grown at 25°C.

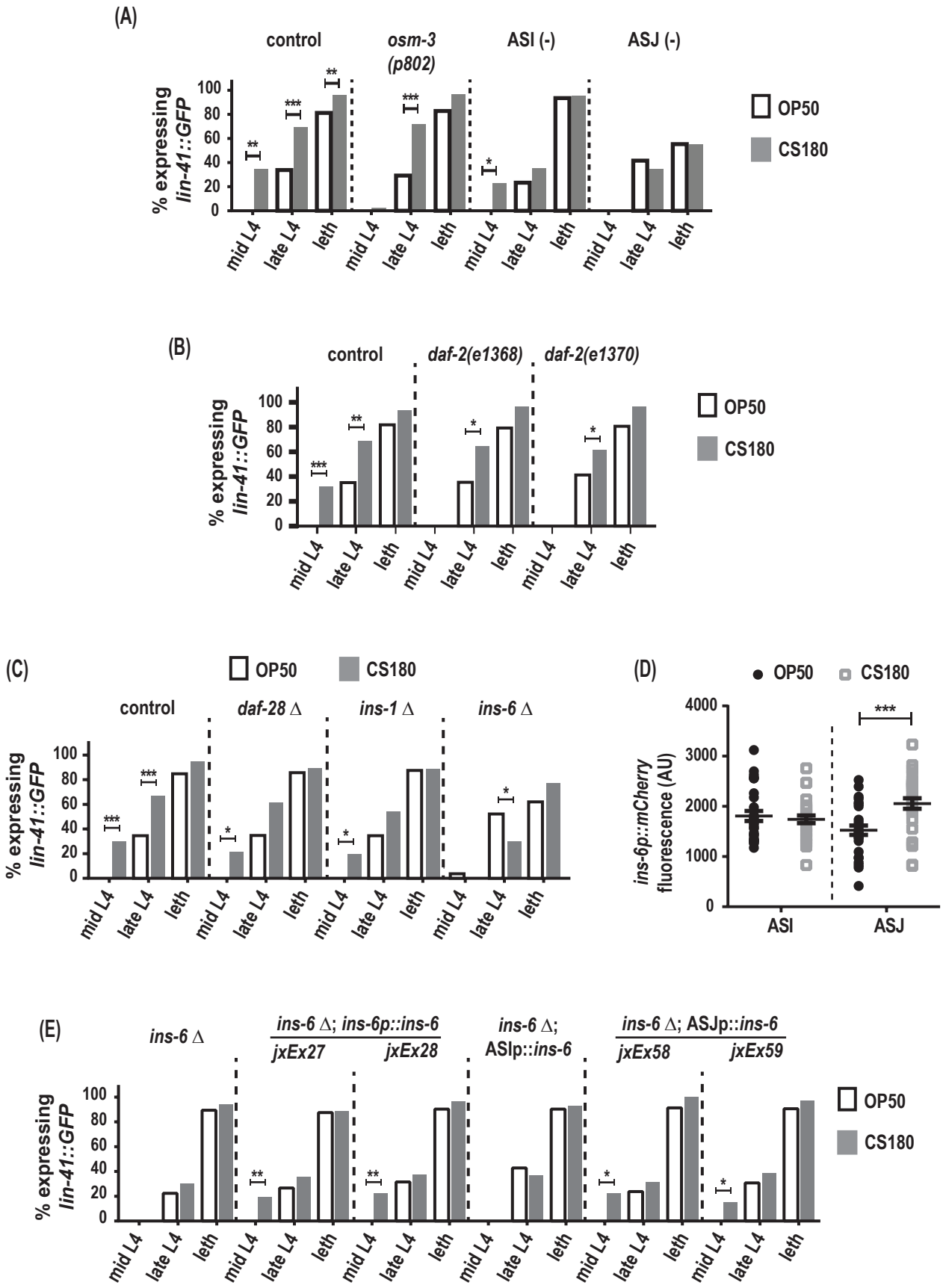
(A)
control
osm-3 (p802)
ASI (-)
ASJ (-)
% expressing lin-41::GFP
OP50
CS180
mid L4
late L4
leth
(B)
control
daf-2(e1368)
daf-2(e1370)
(C)
control
daf-28 Δ
ins-1 Δ
ins-6 Δ
(D)
ins-6p::mCherry fluorescence (AU)
ASI
ASJ
(E)
ins-6 Δ
ins-6 Δ; ins-6p::ins-6
jxEx27
jxEx28
ins-6 Δ; ASIp::ins-6
ins-6 Δ; ASJp::ins-6
jxEx58
jxEx59

Figure 5. *ins-6* acts from the ASJ neurons to promote early onset of oogenesis. (A) Food type-dependent expression of the oogenesis reporter *lin-41::GFP* in control and different sensory mutants. **(B-C)** *lin-41::GFP* expression in *daf-2* reduction-of-function mutants **(B)** and in ILP deletion (Δ) mutants **(C)**. **(D)** *ins-6p::mCherry* transcriptional reporter *drcSi68* expression in ASI (n = 29, OP50; n = 29, CS180) and ASJ (n = 30, OP50; n = 30, CS180) neurons during mid-to-late L3. **(E)** *lin-41::GFP* expression in *ins-6* deletion mutants that were either rescued with: (i) the wild-type *ins-6* genomic locus in two independent lines, *jxEx27* and *jxEx28*; (ii) ASI neuron-specific expression of *ins-6*; or (iii) ASJ neuron-specific expression of *ins-6* in two independent lines, *jxEx58* and *jxEx59*. Because *daf-2* mutants arrest as dauers at 25°C but not at 20°C, controls and *daf-2* mutants in **(B)** were shifted from 20°C to 25°C as early L3s. In contrast, all other animals were continuously grown at 25°C on OP50 (white bars or black circles) or CS180 (grey bars or grey squares). * indicates $p \leq 0.05$; **, $p \leq 0.01$; ***, $p \leq 0.001$; and leth, lethargus.

Figure 5—supplement 1. Statistical analyses of oogenesis onset in different groups of animals on OP50 versus CS180. GFP (+) and GFP (-) are animals that expressed or did not express the *lin-41::GFP* oogenesis marker, respectively. The figure panels associated with the data are indicated. Significant p values are shown in red and italicized. * denotes p values between OP50-fed worms versus CS180-fed worms. # denotes experiments in which animals that carry the *daf-2(e1368)* or *daf-2(e1370)* mutation and the corresponding controls were grown at 20°C and transferred to 25°C at the early L3 stage. All other experiments involved animals that were continuously grown at 25°C.

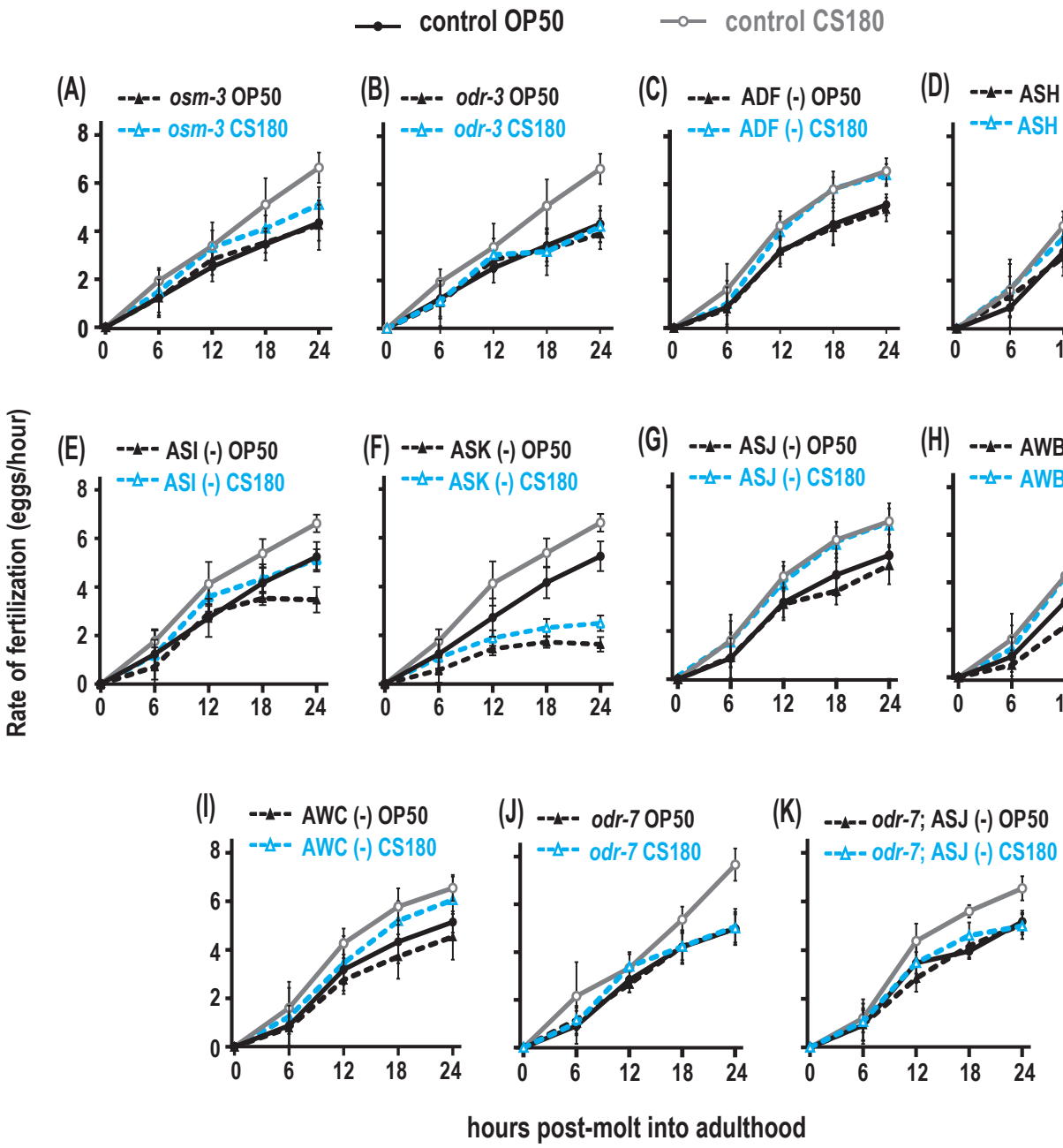
control OP50
control CS180
(A)
osm-3 OP50
osm-3 CS180
(B)
odr-3 OP50
odr-3 CS180
(C)
ADF (-) OP50
ADF (-) CS180
(D)
ASH (-) OP50
ASH (-) CS180
(E)
ASI (-) OP50
ASI (-) CS180
(F)
ASK (-) OP50
ASK (-) CS180
(G)
ASJ (-) OP50
ASJ (-) CS180
(H)
AWB (-) OP50
AWB (-) CS180
(I)
AWC (-) OP50
AWC (-) CS180
(J)
odr-7 OP50
odr-7 CS180
(K)
odr-7; ASJ (-) OP50
odr-7; ASJ (-) CS180
Rate of fertilization (eggs/hour)
hours post-molt into adulthood

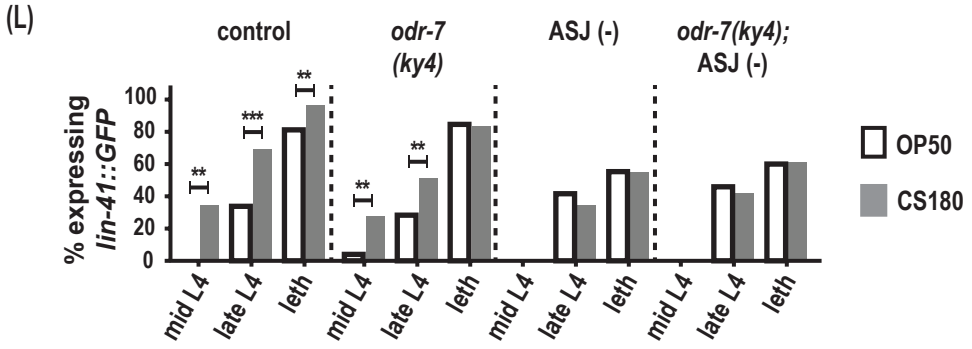
(L)
control
odr-7 (ky4)
ASJ (-)
odr-7(ky4); ASJ (-)
% expressing lin-41::GFP
mid L4
late L4
leth
OP50
CS180

Figure 6. AWA olfactory neurons modulate food type-dependent fertilization rates, but not oogenesis onset. (A-B) Sensory mutations influenced the food-type effects on fertilization rates. **(C-I)** Animals that lack the sensory neurons ADF **(C)**, ASH **(D)**, ASI **(E)**, ASK **(F)**, ASJ **(G)**, AWB **(H)**, and AWC **(I)**. **(J)** Animals lacking the sensory neuron AWA in *odr-7* mutants. **(K)** Animals that lack both AWA and ASJ. Controls for **G** and **K** carried the *ofm-1p::gfp* marker in the wild-type background. All other controls **(A-F, H-J)** were wild-type worms. **(L)** Food type-dependent expression of the oogenesis reporter *lin-41::GFP* in controls or animals lacking AWA and/or ASJ. ** indicates $p \leq 0.01$; ***, $p \leq 0.001$; and leth, lethargus.

Figure 6—supplement 1. Statistical analyses of fertilization rates and oogenesis onset in different sensory-impaired animals on OP50 versus CS180. Sheet 1 shows the analyses for fertilization rates before normalization; sheet 2, for normalized fertilization rates; and sheet 3, for oogenesis onset in animals lacking AWA and/or ASJ. On sheet 1, N is the total number of animals that were assayed. Means are from pooled data from multiple, independent trials. SD is the standard deviation. On sheet 3, GFP (+) and GFP (-) are animals that expressed or did not express the *lin-41::GFP* oogenesis marker, respectively. On all sheets, the figure panels associated with the data are indicated. Significant p values are shown in red and italicized. On sheets 1 and/or 3, the following abbreviation and superscripted letters denote: NA, not applicable; *A*, p values between a given strain grown on OP50 versus CS180 at each time point; *B*, p values between a given strain grown on OP50 versus wild type on OP50; and *C*, p values between a given strain grown on CS180 versus wild type on CS180.

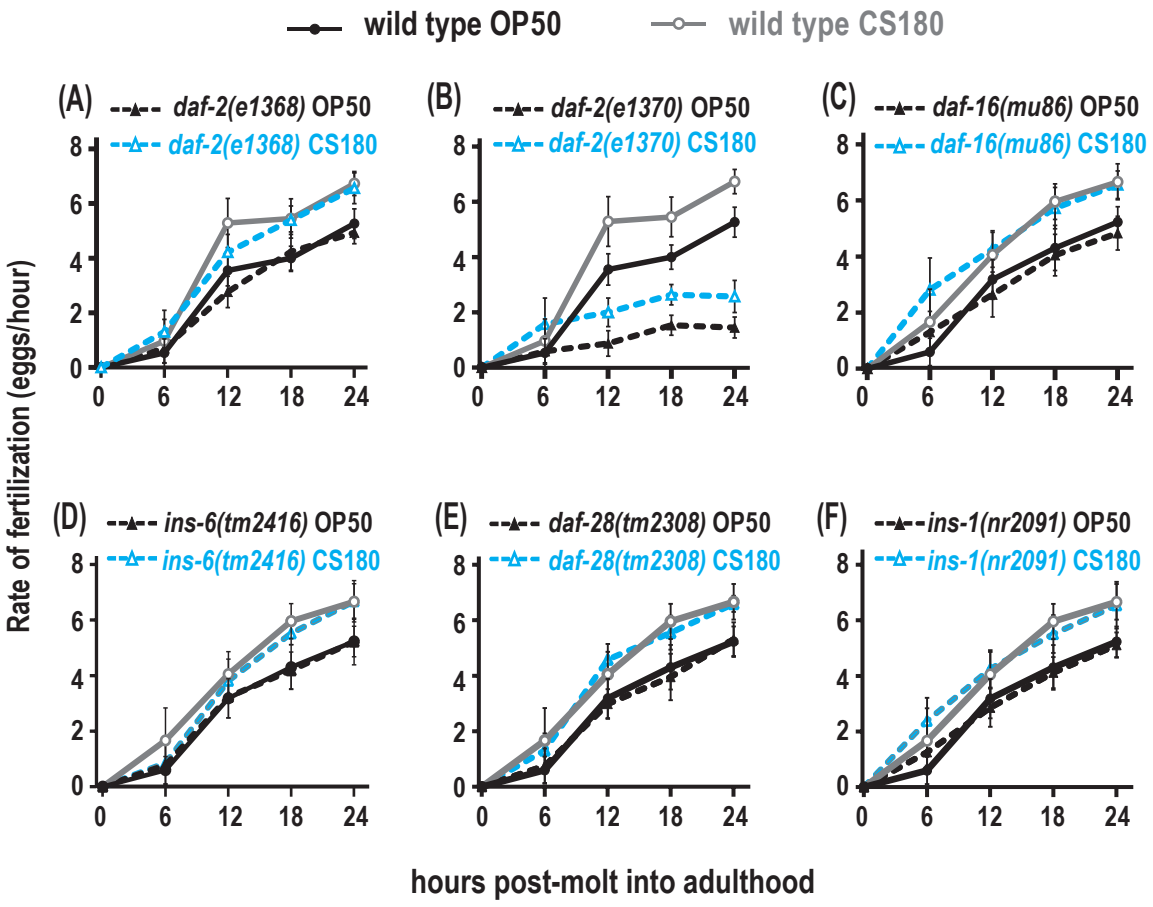
wild type OP50
wild type CS180
(A)
daf-2(e1368) OP50
daf-2(e1368) CS180
(B)
daf-2(e1370) OP50
daf-2(e1370) CS180
(C)
daf-16(mu86) OP50
daf-16(mu86) CS180
(D)
ins-6(tm2416) OP50
ins-6(tm2416) CS180
(E)
daf-28(tm2308) OP50
daf-28(tm2308) CS180
(F)
ins-1(nr2091) OP50
ins-1(nr2091) CS180
Rate of fertilization (eggs/hour)
hours post-molt into adulthood
0
2
4
6
8
0
6
12
18
24

Figure 7. Insulin receptor signaling alter global fertilization rates independent of food type. (A) The weak reduction-of-function *daf-2(e1368)* mutant. **(B)** The strong reduction-of-function *daf-2(e1370)* mutant. **(C-F)** *daf-16* null mutants and the three ILP mutants, *ins-6*, *daf-28* or *ins-1*. Controls and *daf-2* mutants in **(A-B)** were shifted from 20°C to 25°C as early L4s, whereas all other animals were continuously grown at 25ºC on OP50 (black closed circles for wild type; black closed triangles for the indicated mutants) or CS180 (grey open circles for wild type; blue open triangles for the indicated mutants).

Figure 7—supplement 1. Statistical analyses of fertilization rates in insulin signaling-impaired animals on OP50 versus CS180. Sheet 1 shows the analyses for fertilization rates before normalization; and sheet 2, for normalized fertilization rates. N is the total number of animals that were assayed. Means are from pooled data from multiple, independent trials. SD is the standard deviation. The figure panels associated with the data are indicated. Significant p values are shown in red and italicized. [#] denotes experiments in which animals that carry the *daf-2(e1368)* or *daf-2(e1370)* mutation and the corresponding controls were grown at 20°C and transferred to 25°C at the early L4 stage. The following abbreviation and superscripted letters denote: NA, not applicable; *A*, p values between a given strain on OP50 versus CS180 at each time point; *B*, p values between a given strain grown on OP50 versus wild type on OP50; and *C*, p values between a given strain grown on CS180 versus wild type on CS180; *D*, p values between a given strain versus the indicated ILP double or triple mutant on OP50; and *E*, p values between a given strain versus the indicated ILP double or triple mutant on CS180.

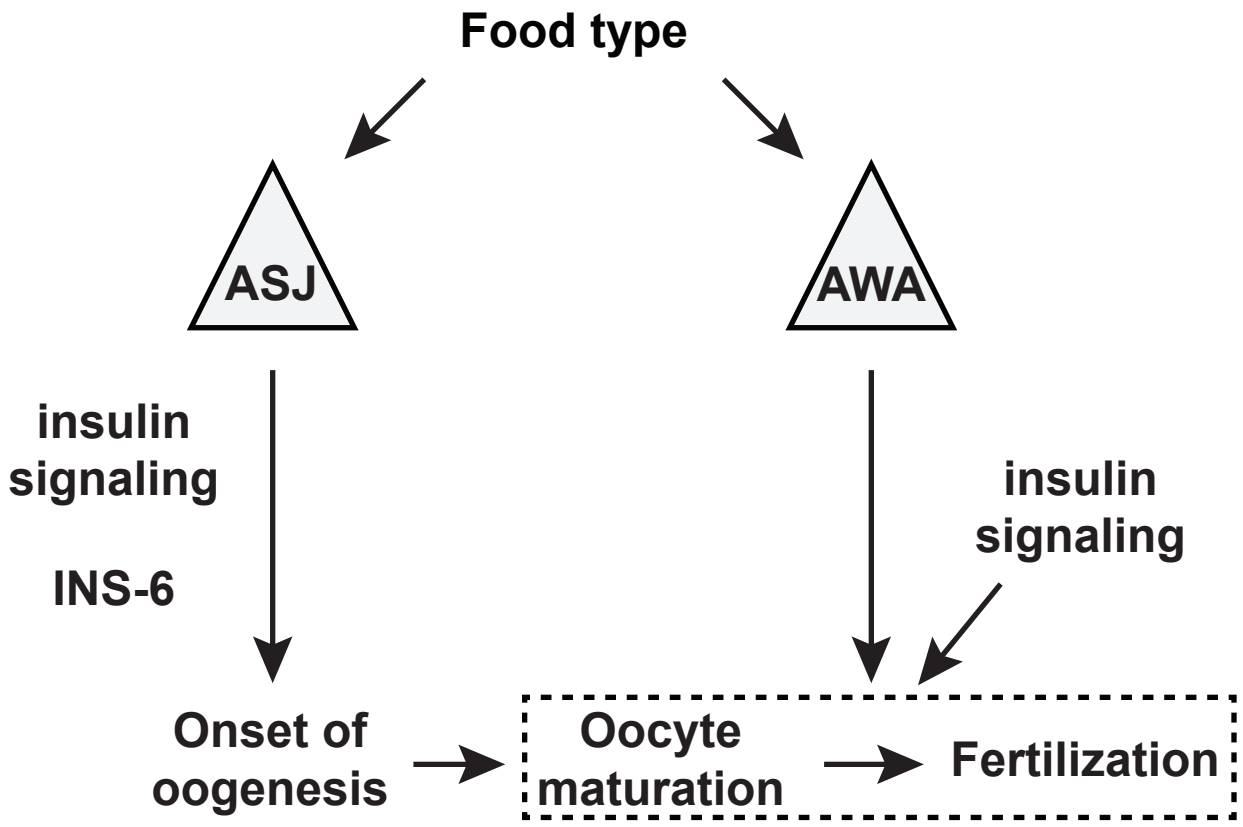
Food type
ASJ
AWA
insulin
signaling
INS-6
insulin
signaling
Onset of
oogenesis
Oocyte
maturation
Fertilization

Figure 8. A model for the sensory modulation of food type-dependent oogenesis onset and fertilization. ILP INS-6 acts from ASJ neurons to promote early onset of oogenesis. Olfactory neuron AWA promotes oocyte fertilization through mechanism(s) distinct from DAF-2 insulin receptor signaling, which in turn regulates fertilization independent of food type through the activities of other insulin-like peptide(s).

Supplementary File 1. List of strains

Strain	Genotype	Reference(s)
Oogenesis marker, *lin-41p::GFP*	*lin-41(tn1541[GFP::tev::s::lin-41])*	Spike et al., 2014
Sensory mutants	*odr-1(n1936)*	L'Etoile and Bargmann, 2000
	odr-3(n1605)	Roayaie et al., 1998
	odr-10(ky225)	Sengupta et al., 1996
	osm-3(p802)	Tabish et al., 1995
	lin-41(tn1541); osm-3(p802)	This work
ADF (-)	*udEx211(srh-142::ced-3(p15); srh-142::ced-3(p17; srh-142::gfp; elt-2::gfp)*	Krzyzanowski et al., 2016
ASH (-)	*peIs1713(sra-6p::mCasp-1 + unc-122p::mCherry)*	Yoshida et al., 2012
ASI (-)	*oyIs84(gpa-4p::TU813 gcy-27p::TU814 gcy-27p::GFP coelp::dsRED)*	Beverly et al., 2011
	lin-41(tn1541); oyIs84	This work
ASJ (-)	*pgIs(trx-1p::ICE)*	Cornils et al., 2011; integrated by M. Goodman (gift)
	lin-41(tn1541); pgIs(trx-1p::ICE)	This work
ASK (-)	*qrIs2(sra-9::mCasp1)*	Srinivasan et al., 2012
AWA (-)	*odr-7(ky4)*	Sengupta et al., 1994
	lin-41(tn1541); odr-7(ky4)	This work
	Ex[odr-10::mCasp1 + myo-3::GFP]	Yoshida et al., 2012; Schiffer et al., 2020
AWB (-)	*peIs1715(str-1p::mCasp-1 + unc-122p::GFP)*	Yoshida et al., 2012
AWC (-)	*oyIs85(ceh-36p::TU#813 + ceh-36p::TU#814 + srtx-1p::GFP + unc-122p::DsRed)*	Beverly et al., 2011
ASJ (-); AWA(-)	*pgIs(trx-1p::ICE); odr-7(ky4)*	This work
	lin-41(tn1541); pgIs(trx-1p::ICE); odr-7(ky4)	This work
Insulin signaling mutants	*daf-2(e1368)*	Gems et al., 1998
	lin-41(tn1541); daf-2(e1368)	This work
	daf-2(e1370)	Gems et al., 1998
	lin-41(tn1541); daf-2(e1370)	This work
	daf-16(mu86)	Lin et al., 1997
	ins-1(nr2091)	Pierce et al., 2001
	lin-41(tn1541); ins-1(nr2091)	This work
	ins-6(tm2416)	Cornils et al., 2011
	lin-41(tn1541); ins-6(tm2416)	This work
	daf-28(tm2308)	Cornils et al., 2011
	lin-41(tn1541); daf-28(tm2308)	This work
	ins-6(tm2416); daf-28(tm2308)	Cornils et al., 2011
	ins-6(tm2416); ins-1(nr2091)	Cornils et al., 2011
	ins-1(nr2091); daf-28(tm2308)	Cornils et al., 2011
	ins-6(tm2416); ins-1(nr2091); daf-28(tm2308)	Cornils et al., 2011
***ins-6* full genomic rescues**	*lin-41(tn1541); ins-6(tm2416); jxEx27(ins-6p::ins-6 [2 ng/ul]; ofm-1::GFP [25 ng/ul])*	Cornils et al., 2011; this work
	lin-41(tn1541); ins-6(tm2416); jxEx28(ins-6p::ins-6 [2 ng/ul]; ofm-1::GFP [25 ng/ul])	Cornils et al., 2011; this work
***ins-6* ASI-specific rescue**	*lin-41(tn1541); ins-6(tm2416); jxEx51(str-3p::ins-6 [25 ng/ul]; ofm-1::GFP [25 ng/ul])*	Cornils et al., 2011; this work
***ins-6* ASJ-specific rescue**	*lin-41(tn1541); ins-6(tm2416); jxEx58(trx-1p::ins-6 [25 ng/ul]; ofm-1::GFP [25 ng/ul])*	Cornils et al., 2011; this work
	lin-41(tn1541); ins-6(tm2416); jxEx59(trx-1p::ins-6 [25 ng/ul]; ofm-1::GFP [25 ng/ul])	Cornils et al., 2011; this work
ins-6p::mCherry drcSi68	*ttTi5605 drcSi68(ins-6p::mCherry; Cb-unc-119[+])II*	This work